The 2009 IEEE/RSJ International Conference on
Intelligent Robots and Systems
October 11-15, 2009 St. Louis, USA

Command Recognition by Haptic Interface on Human Support Robot

Toshiaki Tsuji, *Member*, *IEEE* and Tatsuya Ito

Abstract— **This paper describes a method for command recognition by a haptic interface on a human support robot. Feature quantities are derived from the contact trajectory when an operator runs his finger across the haptic interface. The robot then recognizes a command based on these derived feature quantities from the symbolized contact trajectory. Conforming the robot motion to the symbolized contact trajectory allows for intuitive operation of the robot. The experimental results indicate that novice operators using this interface can obtain high command recognition rates.**

I. Introduction

Recent advances in mechatronics technology raises the expectations for motion control. Specifically, impact relaxation methods have been studied [1], [2], [3] since safety is indispensable on the supposition that human support robots will be put to practical use alongside humans. In these methods, force sensors are often installed on the robots, though conventional force sensors have a small detectable area. The whole body or any part of a human support robot may contact an operator. Therefore, to ensure safety, the method used to detect robot force should cover the entire body of the robot. This is referred to as "whole-body force sensation". This will also be called "whole-body haptic sensation" when it is possible to calculate not only the external force vector but also other information, such as the position of the contact point.

Most of the current examples of whole body haptic sensation use haptic sensors with pressure sensors set in array [4]. On the other hand, methods of applying a single force sensor have also been proposed. Salisbury and Bicchi proposed the idea of intrinsic contact sensing that identifies the contact features on an insensitive end-effector using a 6-axis force sensor [5], [6]. The contact features refer to the point of application of an external force and its force vector. Iwata et al. developed a whole-body haptic interface, applying these theories to human support robots [7]. The authors developed a whole-body haptic sensor, "haptic armor", that does not require the installation of additional wiring or sensors on the outer shell and showed that contact features can be identified by only the force sensor, even for an outer shell with angulated surfaces [8], [9]. An external force observer [10] detects the external force generated on the whole body of the robot, while the point of application of an external force should be known. When these whole-body haptic sensation technologies are introduced into robots, not only is the safety of the robot improved, but the whole body of the robot also works as a haptic interface. For example, Miyashita et al. proposed a system with haptic sensors that recognizes how an operator contacts it and attempted to collect information of haptic communication [11]. Through the application of haptic communication to robot operation, the efficiency of cooperative work will increase under the mechanical interference in strength [12]. Although some researchers are currently studying haptic communication with robots, command recognition based on haptic information remains to be investigated. Command recognition through a haptic interface is a good candidate for multimodal communication, since there is always the possibility of physical interaction between a human support robot and a human.

On the basis of the abovementioned results, this paper describes a method for command recognition by a haptic interface on a robot. The robot derives feature quantities from the contact trajectory when an operator runs his finger across the haptic interface. The robot then recognizes a command based on the derived feature quantities of the symbolized contact trajectory. Intuitive operation can be actualized by conforming the robot motion to the contact trajectory.

Although mouse gesture [13] and some interfaces on video games or music players have already accomplished intuitive interfaces, the effect has not been shown in a robot, a system which actively interacts with humans. This paper also shows that the efficient interface, which allows multidimensional information to be transmitted by a single motion, is produced using force information.

II. Mechanism of haptic interface

A. Structure

The haptic interface mechanism, named "haptic armor" is explained in the example of a mobile robot shown in Fig. 1. The interface is composed of two parts: an end-effector; and a sensor device. The end-effector is merely a constructional material that conveys external force to the sensor device. External force on the end-effector is sensed at the sensor device since the end-effector, the sensor device, and the main body are tightly fixed to each other. The present study uses a commercial 6-axis force sensor as the sensor device. External force can also be measured by directly implementing strain gauges on the end-effector. Whole-body force sensation is realized since the end-effector is shell-shaped.

B. Measurement method

A brief diagram of the force/torque measurement is shown in Fig. 2. External force is detected at the sensor device since

This author was supported in part by the Tateishi Science Foundation.

T. Tsuji and T. Ito are with Graduate School of Science and Engineering, Saitama University, 255 Shimo-ohkubo, Sakura-ku, Saitama 338-8570, Japan

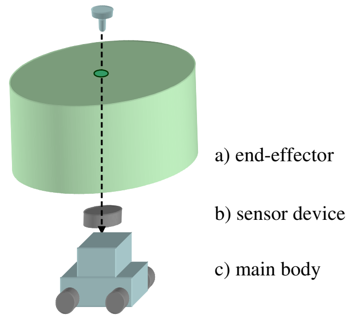

Fig. 1. Mechanism of haptic interface

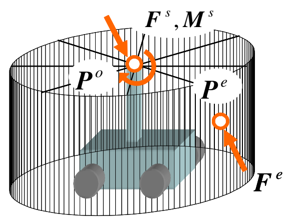

Fig. 2. Force/torque measurement

the force is transmitted through the end-effector. Equation (1) shows the equilibrium of force on the end-effector.

$$\sum_{i=1}^{n} \boldsymbol{F}_i^e + \boldsymbol{F}^s = w^e \ddot{\boldsymbol{P}}^o - w^e \boldsymbol{r}^g \times \ddot{\boldsymbol{\phi}} \quad (1)$$
$$\boldsymbol{r}^g = \boldsymbol{P}^g - \boldsymbol{P}^o.$$

Here, $\boldsymbol{F}$ denotes triaxial force, superscripts e and s denote external force and force acting at the fixed point on the sensor device. n denotes the number of contact points. w^e, $\boldsymbol{P}^o$, $\boldsymbol{P}^g$ and $\ddot{\boldsymbol{\phi}}$ denote weight of the end-effector, the point the end-effector is fixed, the center of mass (COM) of the end-effector, and angular acceleration about the vertical axis, respectively.

At the same time, measured torque on the sensor device corresponds to resultant torque due to external force.

$$\sum_{i=1}^{n} (\boldsymbol{F}_i^e \times (\boldsymbol{P}_i^e - \boldsymbol{P}^o)) + \boldsymbol{M}^s = w^e \boldsymbol{r}^g \times \ddot{\boldsymbol{P}}^o + \boldsymbol{I}^e \ddot{\boldsymbol{\phi}} \quad (2)$$

Here, $\boldsymbol{P}_i^e$ denotes triaxial position of the ith contact point. When distributed pressure acts on a surface, center of pressure substitutes $\boldsymbol{P}_i^e$. $\boldsymbol{M}^s$ is triaxial torque applied on the fixed point. $\boldsymbol{I}^e$ is moment of inertia (MOI) of the end-effector.

C. Calculation of contact point

Haptic armor has an ability to calculate the position of the contact point in the case of a single contact. Assuming that only one contact point exists, (2) is developed as follows:

$$\boldsymbol{F}^e \times (\boldsymbol{P}^e - \boldsymbol{P}^o) + \boldsymbol{M}^o = 0 \quad (3)$$
$$\boldsymbol{M}^o = \boldsymbol{M}^s - w^e \boldsymbol{r}^g \times \ddot{\boldsymbol{P}}^o - \boldsymbol{I}^e \ddot{\boldsymbol{\phi}}. \quad (4)$$

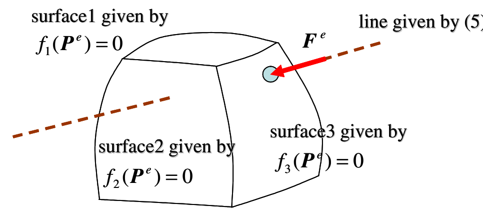

Fig. 3. Diagrammatic representation of (5) and (7)

Equation (3) can be reformed as follows:

$$\begin{aligned} P_z^e &= \frac{-M_x^o - F_z^e P_y^o}{F_y^e} + P_z^o + \frac{F_z^e}{F_y^e} P_y^e \\ &= \frac{M_y^o - F_z^e P_x^o}{F_x^e} + P_z^o + \frac{F_z^e}{F_x^e} P_x^e. \end{aligned} \quad (5)$$

Here, subscripts x, y, z refer to the direction of the Cartesian coordinates. $M_x^o, M_y^o, F_x^e, F_y^e$ and F_z^e are calculated based on the force responses and acceleration responses while P_x^o, P_y^o and P_z^o are derived by direct kinematics. Then (5) shows a straight line collinear with $\boldsymbol{F}^e$. The straight line gives constraints on $\boldsymbol{P}^e$. If the shape of the outer shell is known, position of a contact point $\boldsymbol{P}^e$ can be estimated. Suppose the shape of the outer shell is given by the following equation:

$$f(\boldsymbol{P}^e) = 0. \quad (6)$$

$\boldsymbol{P}^e$ is determined from the solution of simultaneous equations (5) and (6). Equation (5) including five force responses shows that 5-axis of force sensation (3-axis force and 2-axis torque) is required for calculation of the contact location.

Since shape of an outer shell is rarely given by a simple equation, the outer shell is often expressed as a collection of multiple surfaces. Hence, (6) is expanded as follows:

$$f_k(\boldsymbol{P}^e) = 0 \qquad (k = 1, 2, \cdots, p) \quad (7)$$

where p is the number of surfaces.

Assume that the outer shell is a convex hull, two solutions exist in the simultaneous equations. In this case, position of the contact point can be determined to be either of the solutions by assuming that only a pushing force acts on the outer shell. The diagrammatic representation of two equations and their intersections are shown in Fig. 3. It also indicates that $\boldsymbol{F}^e$ acts as a pushing force when its vector is oriented inward on the outer shell.

The command recognition method in the present study is expected to work in various haptic interfaces, such as a pressure sensor array or a touch panel. However, haptic armor was used since it extracts smooth trajectory information with less quantization error of the position.

III. Command Recognition Based on Trajectory of Active-Touch Movement

An image of the command recognition method proposed in this paper is presented in Fig. 4. When an operator runs his finger across the haptic interface of the robot, it recognizes the command content from the contact trajectory of the

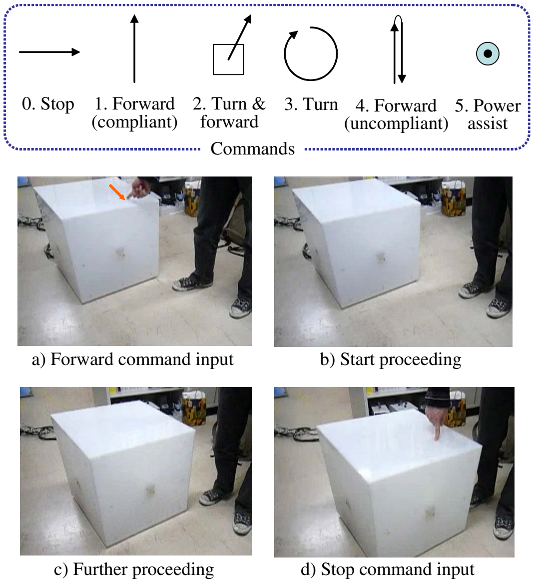

Fig. 4. Image of command recognition

moving finger. The specified motion modes are preset to execute the commands, and then the robot conducts the corresponding operation mode after recognizing the command. In principle, the command can be recognized on all surfaces of an end-effector. However, this paper examines the robot operation modes by using only a top plate, since it is easy for an operator to enter data. The robot recognizes and executes a command in accordance with the following procedures:

- The robot always detects contact with an operator and records the trajectory of the contact point while both of them are touching.
- When contact between the robot and operator is broken, the robot concludes active-touch movement to be completed and derives feature quantities from the contact trajectory.
- The robot recognizes a command based on these derived feature quantities.
- The operation modes are changed based on the command recognition of the robot.

The details of the proposed method are described below.

A. Commands and Corresponding Operation Modes

The present study specifies six types of operation modes. In order for the robot to shift to a desirable operation mode, the patterns of commands symbolized for operation modes must be input. The operation modes are explained as follows:

[Operation mode 1: forward (compliant)] While assuring safety by compliance control, the robot moves ahead at v_l^{cmd}, the command forward speed. The robot shifts to the stop mode after running l_{fw}, the forward distance. The robot is reset to this mode after active-touch movement of more than the threshold distance r_{th} in the moving direction.

[Operation mode 2: turn & forward] After turning by ϕ_{turn}, the turn angle, the robot shifts to mode No. 1 and moves ahead. Safety is assured by the compliance control system. The robot is reset to this mode after active-touch movement of more than r_{th} from the center part of the top plate.

[Operation mode 3: turn] The robot is turned by the command angular velocity v_ϕ^{cmd}. Safety is assured by compliance control. The robot is reset to this mode after tracing a circular arc in the direction the operator desires to turn the robot.

[Operation mode 4: forward (uncompliant)] The robot moves ahead at the command speed v_l^{cmd} with disturbances such as external force prevented by position control. The robot shifts to the stop mode after running the forward distance l_{fw}. In order to make the robot reset to this mode, an operator has to trace a reciprocating trajectory longer than r_{th}.

[Operation mode 5: power assist] Power assist control is performed with force control. In order to make the robot reset to this mode, it is necessary to continuously contact the range R_{th} for the threshold time t_{th} or more. When an object is placed on the robot, or when the finger of an operator touches the robot, the robot recognizes a command in both cases.

[Operation mode 0: stop] The robot continues to keep its current position under the position control. The robot is reset to this mode after active-touch movement in the lateral direction. However, the robot is also reset to this mode when an operator carries out an input that does not conform to the abovementioned command patterns.

B. Acquisition of Contact-Point Trajectory and Derivation of Feature Quantities

In the proposed method, the contact point and force are recorded in a time series while an operator contacts the robot, and several feature quantities are derived based on the trajectory of these factors. The relationship between the trajectory and the feature quantities is shown in Fig. 5. $\boldsymbol{P}_s$ and $\boldsymbol{P}_f$ denote the start point and the final point, respectively. r, R, S, ψ are the distance between the two points, the maximum distance from the start point, the integral of velocity moment of the contact point, and the angle of the segment connecting the two points, respectively. $\boldsymbol{P}^e(t)$ denotes the contact point $\boldsymbol{P}^e$ at the time of t. Based on the start time t_s and final time t_f of contact, the contact time: $t_c = t_f - t_s$ is derived and used as a feature quantity.

Other feature quantities and their calculation methods are described below.

[r: Distance between two points] This is a distance between the start point $\boldsymbol{P}_s$ and the final point $\boldsymbol{P}_f$. It is calculated from (8):

$$r = |\boldsymbol{P}_f - \boldsymbol{P}_s| \tag{8}$$

where, $|\cdot|$ denotes vector length or scalar absolute value.

[R: Maximum distance from start point] This expresses the length up to a point that is the maximum distance from the start point $\boldsymbol{P}_s$ and is calculated from (9):

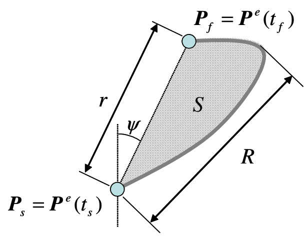

Fig. 5. Contact trajectory

$$R = \max\{r(t)|t_s < t \le t_f\} \tag{9}$$
$$r(t) = |\boldsymbol{P}^e(t) - \boldsymbol{P}_s|$$

[S: Integral of velocity moment of contact point] S is calculated from (10):

$$S = \frac{1}{2}\int_{t=t_s}^{t_f} \boldsymbol{P}^e(t)\times\boldsymbol{V}^e(t) + \frac{1}{2}\boldsymbol{P}_f\times(\boldsymbol{P}_s - \boldsymbol{P}_f) \tag{10}$$

where, $\boldsymbol{V}^e(t)$ is the traveling speed at the contact point. This is calculated on the time derivate of $\boldsymbol{P}^e(t)$. As shown in (10), S is the integral of the velocity moment of the contact point. It may be a negative value depending on the direction of the inflective trajectory. Using this feature makes it possible to recognize the turning direction of the contact trajectory based on S.

[ψ: Angle of segment connecting two points] The angle of segment ψ is calculated from (11):

$$\begin{cases} \psi = \tan^{-1}\frac{P_{fx}-P_{sx}}{P_{fy}-P_{sy}} & (P_{fy} > P_{sy}) \\ \psi = \frac{1}{2}sign(P_{fx}-P_{sx})\pi & (P_{fy} = P_{sy}) \\ \psi = \tan^{-1}\frac{P_{fx}-P_{sx}}{P_{fy}-P_{sy}} & \\ \qquad +sign(P_{fx}-P_{sx})\pi & (P_{fy} < P_{sy}) \end{cases} \tag{11}$$

C. Algorithm of Command Recognition

The flowchart for command recognition is shown in Fig. 6. This algorithm starts at the completion of the active-touch movement, transmits the command recognition number N_{com}, and finally calculates the command execution parameters. The feature quantity S is derived to determine whether the contact trajectory is linear or not. On the other hand, r and R values determine whether the reciprocating trajectory is performed or not. The trajectory angle ψ, contact time t_c, and start point $\boldsymbol{P}_s$ are used as the evaluation standards for command recognition. The execution parameters of each command recognized in the above conditional branches are presented in Table I. The forward operation mode 1 and mode 4 shall be given the command speed v_l^{cmd} in proportion to active-touch movement speed $\frac{r}{t_c}$ and the forward distance l_{fw} shall be proportioned to the distance r. The turn angle ϕ_{turn} in operation mode 2 shall correspond to the angle of segment ψ. The turn speed in operation mode 3, which is inverse proportional to time t_c, shall conform to the active-touch movement speed. Intuitive operation can be actualized by conforming the robot motion to the active-touch movement as previously mentioned.

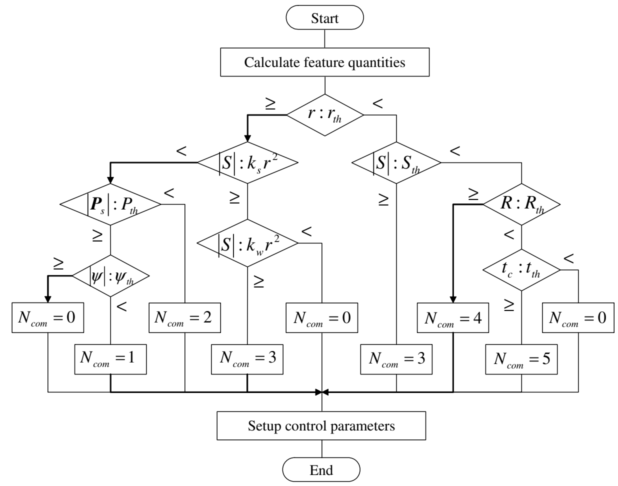

Fig. 6. Flow chart for command recognition

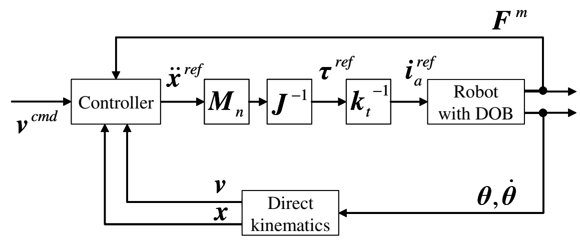

Fig. 7. Block diagram of control system

One of the advantages of command recognition using haptic interface is that multidimensional information can be transmitted by a single motion. For example, when issuing the command to make the robot turn and move ahead, the command number ($N_{com} = 2$) and three-dimensional parameters (turn angle ϕ_{turn}, forward distance l_{fw}, forward command speed v_l^{cmd}) are transmitted by a single motion. Since this study uses information based on the contact trajectory and can also apply information of the external force vector, there is a possibility to further increase the transmittable information volume.

D. Structure of Control System

The block diagram of the control system is shown in Fig. 7. This control system, based on the disturbance observer [14], has the feedback loops of force, position and speed. Three types of controllers can be selected for use as the operation modes of this system. The controller described in Fig. 7 is switchable and the applicable controllers are shown in Fig. 8. Here, $\boldsymbol{k}_f = diag(k_{fl}\ k_{f\phi}), \boldsymbol{k}_p = diag(k_{pl}\ k_{p\phi}), \boldsymbol{k}_v = diag(k_{vl}\ k_{v\phi}), \boldsymbol{M}_n$ and $\boldsymbol{k}_t$ present force-, position- and speed-control gains, nominal inertia matrix and motor torque constant, respectively. $\boldsymbol{F}^m = [F_y^e\ M_z^o]$ is set to collect only the components, which affect the motion of the traveling robot, from among the external forces $\boldsymbol{F}^e$ and $\boldsymbol{M}^o$ detected by the haptic interface. When the operation mode is changed, the command value must be

TABLE I

CONTROLLER AND PARAMETERS OF EACH COMMAND

Command	N_{com}	Controller	v_l^{cmd}	v_ϕ^{cmd}	l_{fw}	ϕ_{turn}
Stop	0	Position controller	0	0	—	—
Forward(compliant)	1	Compliance controller	$k_{fw}\frac{r}{t_c}$	0	$k_l r$	—
Turn & Forward	2	Compliance controller	0	$\frac{2\pi}{t_r}sign(\psi)$	—	ψ
Turn	3	Compliance controller	0	$\frac{k_\phi}{t_c}$	—	—
Forward(uncompliant)	4	Position controller	$k_{fw}\frac{r}{t_c}$	0	$k_l r$	—
Power Assist	5	Force controller	0	0	—	—

compensated to prevent discontinuous input from switching these controllers.

IV. EXPERIMENT

A. Experimental setup

An overview of the experimental setup is shown in Fig. 9. Although it is a mobile robot with two simple wheels, the proposed method can be applied to omni-directional wheels as well. The main body with a sensor device in the left figure is covered with a cubic end-effector. The bottom of the cube is open for ground contact. The elements and parameters of the robot are listed in Table II.

B. Results of Command Recognition

The results of command recognition by an actual robot are described below. The response and contact trajectory during command transmission based on active-touch movement are shown in Figs. 10 and 11. The result when operation mode forward (compliance control) was commanded twice is shown in Fig. 10. The square area drawn in the upper part of figure represents the top plate of the haptic armor, and the black line represents the contact trajectory. In addition, the vertical dotted lines in the graph indicate the time when the operation mode was switched. Active-touch movement was performed so that the contact point moves in accordance with the robot running direction in both cases. When the second command was issued by an active-touch movement of a long trajectory in a short time, the forward traveling distance of the robot increased and its speed also increased compared to that of the first command. These results indicated that the forward traveling distance and speed of the robot can be adjusted intuitively based on the active-touch movement trajectory.

The result when turn & forward, turn, and stop were commanded in order is shown in Fig. 11. When active-touch movement was performed to $\frac{1}{4}\pi$ in the right from the center point of the top plate of the haptic armor, the robot turned to almost $\frac{1}{4}\pi$ in the right and moved ahead. Next, when a half circle was traced clockwise, the robot recognized a turn command and started to turn clockwise. When active-touch movement was performed in the lateral direction following the turn command, the robot recognized the command and stopped its motion. The parameters used in this experiment are presented in Table III.

C. Evaluation of Command Recognition Rate

Command recognition rate was evaluated for all command input patterns, and the results of a test for 8 beginners and 2 skilled operators are presented in Table IV. The skilled operators were trained in use of the command recognition system using the haptic interface for 20 min. The evaluation of the beginners was made after they received an explanation of the method for inputting commands and attempted to enter the commands one at a time. The mean command recognition across all users was over 98%. These results indicate that the interface is highly efficient for both skilled operators and beginners.

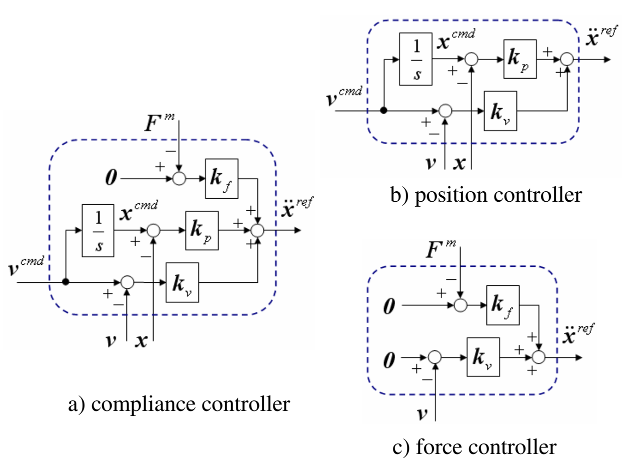

Fig. 8. Block diagram of controller in each mode

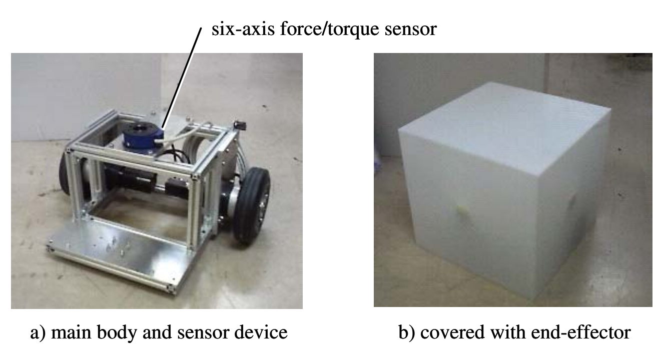

Fig. 9. Experimental system

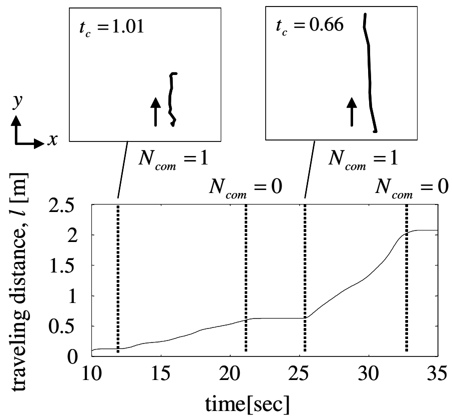

Fig. 10. Command recognition of forward(compliance)

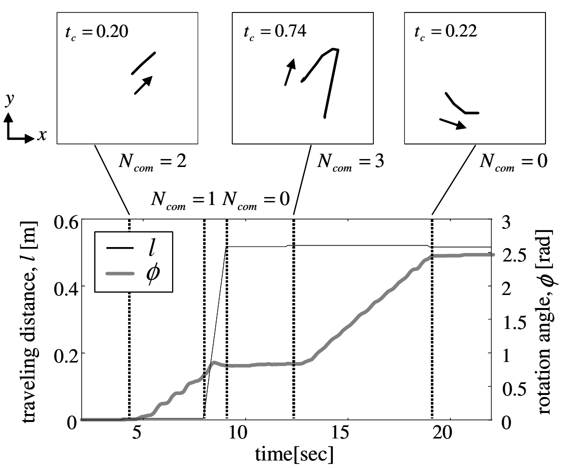

Fig. 11. Command recognition of turn & forward

V. Conclusion

This paper describes a method of command recognition by a robot using a haptic interface. In this method, the robot derives feature quantities from the contact trajectory when an operator runs his finger across the haptic interface, and the robot recognizes a command based on the derived quantities. Conforming the robot motion to the symbolized contact trajectory actualizes intuitive operation. The experimental results indicate that the haptic sensing mechanism is a good candidate as a highly efficient interface.

References

[1] J. Urbano, K. Terashima, T. Miyoshi, H. Kitagawa: "Impedance control for safety and comfortable navigation of an omni-directional mobile wheelchair," *Proc. 2004 IEEE/RSJ Int. Conf. on Intelligent Robots and Systems (IROS 2004)*, Vol. 2, pp. 1902–1907, 2004.

[2] Y. Shoji, M. Inaba and T. Fukuda: "Stable Contact Control of Robotic Manipulator Based on Unified Approach," *J. Robot. Soc. Jpn.*, Vol. 11, No. 5, pp. 77–91, 1993.

[3] E. Ohashi, T. Aiko, T. Tsuji, H. Nishi, K. Ohnishi: "Collision Avoidance Method of Humanoid Robot With Arm Force," *Trans. on Ind. Electron.*, Vol. 54, No. 3, pp. 1632–1641, 2007.

[4] Y. Yamada, T. Morizono, Y. Umetani: "Highly Soft Viscoelastic Robot Skin With a Contact Object-Location-Sensing Capability," *IEEE Trans. Ind. Electron.*, Vol. 52, No. 4, pp. 960–968, 2005.

[5] J. Salisbury: "Interpretation of contact geometries from force measurements," *Proc. of the IEEE Int. Conf. Robotics and Automation*, pp. 240–247, 1984.

[6] A. Bicchi: "Intrinsic Contact Sensing for Soft Fingers," *Proc. of the IEEE Int. Conf. Robotics and Automation*, pp. 968–973, 1990.

[7] H. Iwata and S. Sugano: "Whole-body Covering Tactile Interface for Human Robot Coordination," *Proc. of the IEEE Int. Conf. Robotics and Automation*, pp. 3818–3824, 2002.

[8] T. Tsuji, Y. Kaneko, S. Abe: "Whole-Body Force Sensation by Robot with Outer Shell," *Proc. of the IEEE Int. Workshop on Advanced Motion Control (AMC'08)*, pp. 365–370, 2008.

[9] T. Tsuji, Y. Kaneko, S. Abe: "Whole-body Force Sensation by Force Sensor with Shell-shaped End-effector," *IEEE Trans. Ind. Electron.*, Vol. 56, No. 5, pp. 1375–1382, 2009.

[10] T. Murakami, F. Yu, K. Ohnishi: "Torque Sensorless Control in Multidegree-of-Freedom Manipulator," *IEEE Trans. Ind. Electron.*, Vol. 40, No. 2, pp. 259–265, 1993.

[11] T. Miyashita, T. Tajika, H. Ishiguro, K. Kogure, and N. Hagita: "Haptic Communication between Humans and Robots," *Proc. of 12th Int. Symp. Robotics Research*, 2005.

[12] K. B. Reed, M. Peshkin, M. J. Hartmann, J. Patton, P. M. Vishton, M. Grabowecky: "Haptic Cooperation Between People, and Between People and Machines," *Proc. of the IEEE Int. Conf. Intelligent Robots and Systems*, pp. 2109–2114, 2006.

[13] M. S. Dulberg, R. St. Amant, L. S. Zettlemoyer: "An Imprecise Mouse Gesture for the Fast Activation of Controls," *Proc. INTERACT'99*, pp. 375–382, 1999.

[14] K. Ohnishi, M. Shibata, T. Murakami: "Motion Control for Advanced Mechatronics," *IEEE/ASME Trans. Mechatronics*, Vol. 1, No. 1, pp. 56–67, 1996.

[15] Y. Hirata, K. Kosuge, T. Oosumi, H. Asama, H. Kaetsu, K. Kawabata: "Coordinated Transportation of a Single Object by Omni-Directional Mobile Robots with Body Force Sensor," *J. Robotics and Mechatronics*, Vol. 12, No. 3, pp. 242–248, 2000.

TABLE II

Elements of Experimental System

Actuator	Yaskawa SGMAS-A5A(AC50W)
Motor driver	Yaskawa SDGA-A5BS
Force sensor	Nitta IFS 67M25A50-I40-ANA
Size	500×500×500 [mm]
Material of outer shell	3 mm acrylic board

TABLE III

Parameters in Experiment

k_{fw}	Scale factor for forward velocity	1.0	
k_l	Scale factor for travel distance	3.0	
k_ϕ	Scale factor for rotation angle	0.2	
t_r	Time period for rotation	4.0	[sec]
k_s	Area ratio threshold for turn mode	0.2	
r_{th}	Threshold of distance r	0.06	[m]
R_{th}	Threshold of maximum distance R	0.07	[m]
S_{th}	Threshold of S for turn mode	0.01	[m^2]
t_{th}	Time threshold for power assist mode	0.01	[sec]
P_{th}	Radius of center circle	0.1	[m]
ψ_{th}	Angle threshold for forward mode	0.46	[rad]

TABLE IV

Command Recognition Results

input command	recognized result 0	1	2	3	4	5	recognition rate [%]
0	180	0	1	0	0	2	98.4
1	1	129	1	0	0	0	98.5
2	1	1	129	0	0	0	98.5
3	0	0	0	131	0	0	100.0
4	1	1	0	7	122	0	93.1
5	1	0	0	0	0	130	99.2